Fabrication a novel 3D tissue engineering scaffold of Poly (ethylene glycol) diacrylate filled with Aramid Nanofibers via Digital Light Processing (DLP) technique

A.Nurulhuda
Quality Engineering, Universiti Kuala Lumpur, Malaysian Institute of Industrial Technology, Malaysia
**nurulhuda@unikl.edu.my*

I. Sudin, Nor Hasrul Akhmal Ngadiman*
School of Mechanical Engineering, Universiti Teknologi Malaysia, Malaysia
izman@utm.my, norhasrul@utm.my

ABSTRACT

The aim of tissue engineering scaffold fabrication is to imitate the structural and mechanical properties of bone as close as possible. However, the selection of optimum scaffold fabrication method becomes challenging due to a variety of manufacturing methods, existing biomaterials and technical requirements. Although a lot of traditional fabrication methods can be used to produce scaffold, unfortunately, each of the conventional methods has lots of limitations. In this experimental study, the researcher has come out with a new approach technique via DLP-3D printing process in fabrication a novel tissue engineering scaffold Poly (ethylene glycol) diacrylate (PEGDA) filled with Aramid Nanofiber (ANFs). In this work, the researcher has proved the potential and capability of these novel composition biomaterial PEGDA/ANFs to be print via DLP-3D printing technique to form a 3D structure which is not yet been established and has not reported elsewhere.

Keywords: *Biomaterial; Biopolymer composite; Additive manufacturing; 3D printing.*

ISSN 1823- 5514, eISSN 2550-164X

Received for review: 2019-04-18
Accepted for publication: 2019-07-18
Published: 2020-06-30

Introduction

Organ or tissue failure due to trauma or aging is a significant health concern because it is expensive and devastating. Nowadays, technology transplantation from one individual into another has faced a significant problem to access enough tissue and organs for all patient [1]. Also, the problem with the immune system with has higher tendency produce chronic rejection and destruction over time [2]. The constraints have contributed to a need for a new solution to provide needed tissue. This led to the development of tissue engineering (TE) to create biological substitutes for repairing or replacing failed organs and tissues [3]-[6].

Tissue engineering has gained more attention in the last decade due to its high success in enabling tissue regeneration. The tissue engineering field utilizes engineering, life and clinical knowledge to address critical tissue loss and issues with organ failure [3], [6], [7]. Tissue engineering also aims to produce patient-specific biological substitutes to circumvent the limitations of present clinical treatments for damaged tissue or organs. These constraints include donor organ shortages, chronic dismissal and cell morbidity [1].

Tissue engineering scaffolding technology offers a temporary template for biological replacement development, maintenance or enhancement of the tissue function or damage to the entire organ [8]–[10]. Tissue engineering technology is unique by offering three-dimensional environments for particular signalling molecules capable of tissue settings [11], [12]. The scaffolds can be either natural, synthetic or hybrid [10]. Tissue engineering technique has the ability to produce organs and tissues. It involves in vitro seeded human cells that are connected to a scaffold. Then these cells proliferate, migrate and distinguish between the particular tissues and recover damaged tissues [13]-[15].

The main objective during scaffold development is to imitate the bone's structural and mechanical features as carefully as possible [16]. The scaffold manufacturing method should, therefore, be versatile to construct biomimetically designed scaffold architectures. Standard methods are generally used to build tissue engineering scaffolds. Several traditional methods used to construct tissue engineering scaffolds are moulding technique, solvent casting, and particulate leaching, gas foaming, and electrospinning [17], [18]. Although lots of conventional fabrication methods can be used to produce scaffold, unfortunately, each of these methods has limitations which they are not able to the internal topology and architecture [10], [14]. To the best of our knowledge, none of the traditional methods is satisfactory to produce scaffolds with fine control dimensions architecture, porosity, and faced with the difficulty of mimicking natural tissue biological function [7], [10], [14], [19].

Alternatively, to conventional manufacturing methods for scaffolds, additive production techniques have recently been developed in tissue

engineering, such as the rapid prototype by which various, precisely formed layers sequentially produce a 3D scaffold. [20]. Subia et al., (2010) has claimed that rapid prototype technique (RP) has drawn tremendous attention with its potential to overcome most of the limitations faced by a conventional technique for fabrication 3D scaffolds [21].

Therefore, the present work in this research study is aim to come out with new approached 3D printing technique via Digital Light Processing (DLP) in fabrication a novel biomaterial PEGDA filled with ANFs which has not been reported elsewhere. The composition of new biomaterial, feasible printing parameter and their mechanical properties are also discussed detail in this work.

Methodology

Resin Preparation

PEGDA in solid form with molecular weight average Mn 700 was dissolved in Dimethyl sulfoxide (DMSO) to get solution with concentrations of 30% wt. Aramid Nanofiber (ANFs) has been synthesized based on the method reported by Guan et al., (2017). The solution was then magnetically stirred continuously for one week at room temperature until a dark red ANF/DMSO dispersion (2.0 mg/ml) was finally obtained. Figure 1 shows steps involved to split bulk Kevlar fibers into aramid nanofibers by deprotonation (removal a hydrogen cation, H+) in the solution of DMSO and KOH.

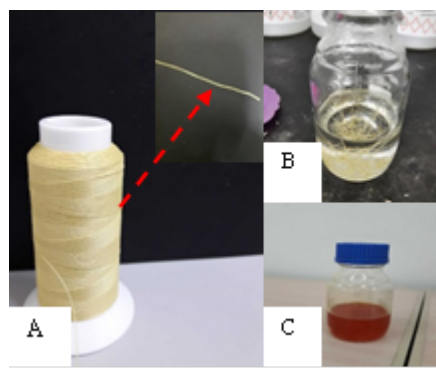

Figure 1: (a) Bulk Kevlar, (b) Kelvar dissolved in DMSO and KOH, (c) orange coloured of ANF dispersion after stirred one at room temperature.

Fabrication 3D Tissue Engineering Scaffold

SolidWorks 3D software was used to model scaffold structure design with a constant value at of porosity, cell size and the total number of unit cell based on the previous literature as shown in Table 1. Design structure with 79% of porosity were said capable to produce higher elastic modulus of scaffold which high porosity is important to heal the bone as regeneration surface area for bone is increased [22]

Table 1: The unit size of scaffold [22]

Parameters	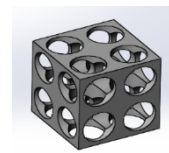
Lattice Name	Lattices with 8 of unit cells
Cell Size (l/d=1.25)	l=10, d=8
Total number of unit cell	8
Porous scaffold volume (mm^3)	1728.82
Porosity (%)	79

The concentration of Diphenyl (2,4,6-trimethylbenzoyl) phosphine oxide (TPO) photoinitiator used has been varied with the aims to initiate the crosslinking process of photopolymerization under DLP 3D printing. Composition of bio-resin PEGDA: TPO (8:2) and ratio for bio-resin to ANFs (9:1) were fixed along with the experiment. In order to identify the effect of photoinitiator concentration on 3D profile formation, experiment has been conducted by varying the concentration of TPO at 0.5, 1.0 and 1.7 %wt. Result of the printed profile was recorded and compared as in Figure 2.

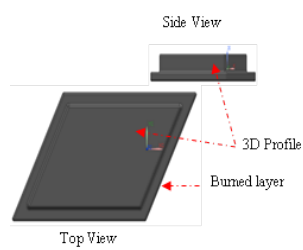

Figure 2: Calibration printing 3D profile

Curing time for calibration printing are setup within range 20s up to 180 s. Result of calibration printing was observed in detail to get the accurate dimension of the 3D profile with dimension 3mm thickness and 5mm width. The aims of the calibration printing process are to get feasible curing time setting for each concentration variation TPO. Detailed process flow diagram for manufacturing 3D tissue engineering PEGDA/ANFs illustrated in Figure 3.

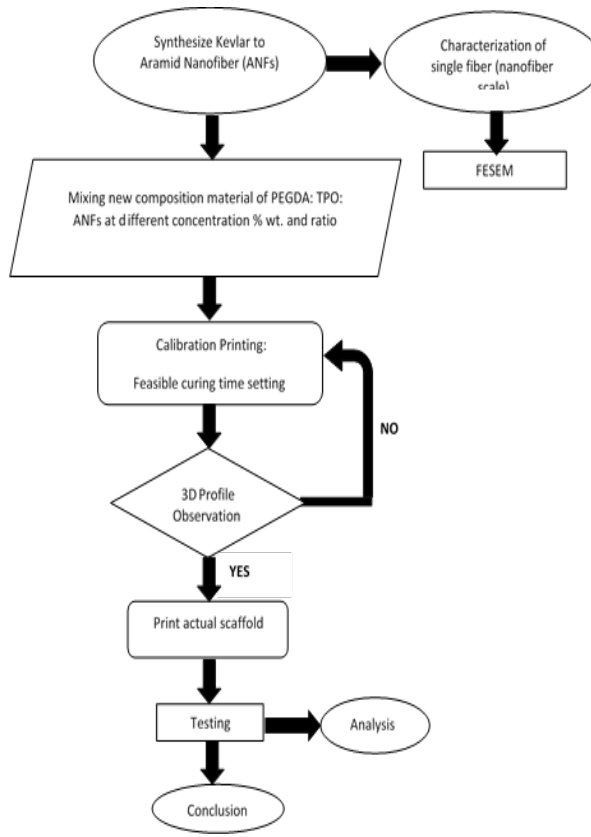

Figure 3: Flow chart of fabrication 3D tissue engineering

Mechanical Test

Compression tests perpendicular to the scaffold plane were conducted. The 3D scaffold PEGDA/ANFs was designed in a cylindrical shape (diameter: 0.5 inches; height: 4mm) according to ASTM standard D695 and printed by DLP 3D printing. Compression test was performed using Shimadzu Machine at testing speed 1 mm/min at room temperature. At least three samples measurement were performed to confirm the reproducibility of data. Stress-strain curves of the printed scaffold were plotted. Young's modulus value was obtained by fitting a line against a linear region of the data [23]. The stress-strain curves were drawn and the Young's modulus value was acquired by providing a line against a linear region of the data [24], [25].

In vitro Biocompatibility Test

Cytocompatibility study of PEGDA/ANFs scaffold was evaluated as described in standard ISO10993-5. 1x105 cells were seeded in 96 well plates overnight and cultured till 80% confluence. The scaffold sample was prepared (1 cm diameter x 0.5 mm thickness). The hydrogel extract was diluted with DMEM, and samples were incubated for 24 h. The solutions in the wells were removed after the incubation period and substituted with a new medium. Subsequently, 20 mL of MTT reagent in PBS was added to each well and the plates were shaken slowly and then incubated at 37 ° C in 5% CO2 for 4 hours. Following incubation, the supernatant has been aspired and 200 mL of DMSO has been added to each well for 30 minutes. Using ELISA microplate reader, the absorption of solubilized formazan product (dark blue) was then evaluated at 570 nm.

Results and Discussion

Microstructure Analysis of Dried ANFs

ANFs in solution phase was dried in the oven to get a nanofiber mat. The morphology of ANFs was characterized under Field Emission Electron Microscope (FESEM) images. Figure 4 shows the Kevlar bulk macroscale was effectively segregated by the principle of deprotonation into aramid nanofibers. The splitting of Kevlar macroscale fibers into nanoscale occurred by abstraction of amide reactive hydrogen and hydrogen bond interaction between polymer chains facilitating ANFs formation. The obtained diameter of single ANFs is at range ~ 30 nm.

Effect Concentration %wt. of TPO on 3D Profile Printing

The results effect of photoinitiator concentration on 3D profile formation were recorded as in Figure 5. Referring to result, it was observed that high concentration TPO (1.7 %wt.) was caused the formation of a thin layer printed profile. The thin layer formation of the 3D profile is due to localization of high

free radical initiation closer to the surface which caused the penetration depth of the photon's laser decreased then produced in a tightly cross-linked and thin cured profile. The result of a repeated experiment at constant value ratio of % wt. PEGDA, TPO and ANFs with lower concentration TPO; 0.5 %wt. and 1 %wt. shown a clear and thick-3D profile cure formed is desirable at a lower initiator concentration 0.5% wt.

Figure 4: Diameter size of single ANFs under FESEM observation

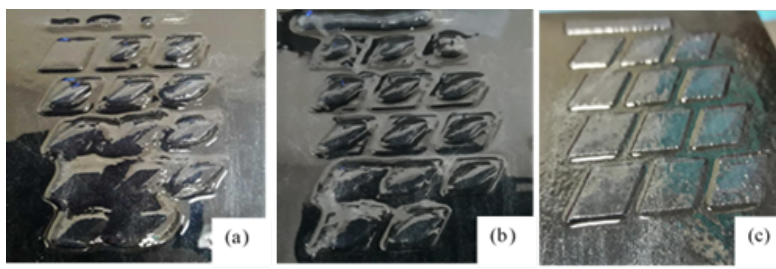

Figure 5: Calibration printing profile resin: ANFs at constant 30% wt PEGDA with varied concentration of TPO; (a) 0.5 %wt, (b) 1.0 %wt and (c) 1.7 %wt.

However, the dimension accuracy of printed profile for 0.5 % wt was formed non-uniform and not consistence between each profile. On the other hands, higher curing time setting for 0.5 % wt TPO was also observed to cause inaccurate dimension. Therefore, it can be concluded that 1.0 % wt concentration of TPO is said to have much accurate size of printed profile

compare than 0.5 % wt and capable to be print perfectly in 3D profile as fast as the 70s.

Young's Modulus Value

The compression test was performed to evaluate the mechanical properties of printed PEGDA/ANFs 3D scaffold. The mechanical value result will determine the strength of the scaffold. The Young's modulus value was recorded and obtained from Stress-strain curved plotted (Figure 6). Based on the result, PEGDA/ANFs scaffold for ratio composition 9:1 was performed their strength value up to 0.17 MPa which correlates to an approximately 88.8 % higher stiffness compare than pure PEGDA scaffold which shows only 0.09 MPa. The used of nanofillers will simultaneously improve the stiffness and toughness of the polymer. Nanofiller polymeric resin also was found to be an efficient way to enhance the mechanical properties of polymeric composites.

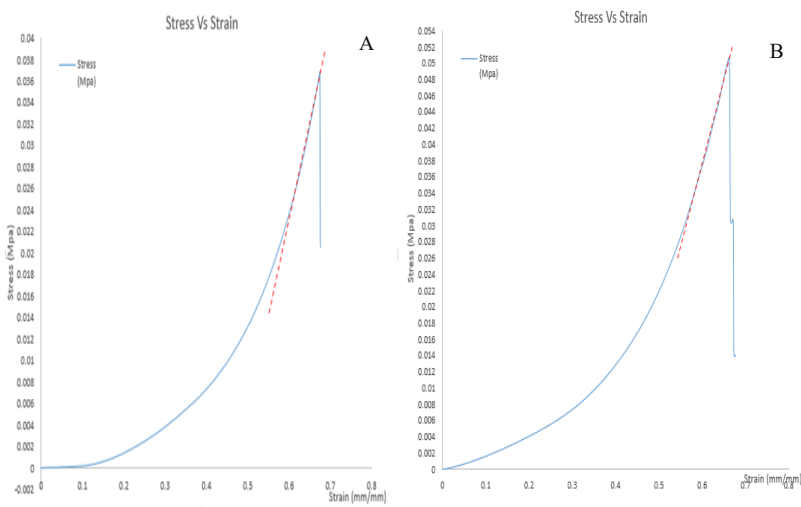

Figure 6: Young's modulus plotted graph of printed scaffold; (A) Pure PEGDA scaffold, (B) PEGDA/ANFs at ratio 9:1.

Biocompatibility of PEGDA/ANFs Scaffold

The extent of cytotoxicity from every composition resin to ANFs was quantified and recorded. By referring to ISO 10993-5, percentages of cell viability above 80% are considered as non- toxic within 80%–60% weak; 60%–40% moderate and below 40% strong cytotoxicity respectively [26], [27]. As indicated in Figure 7, the percentage of cell viability for the printable PEGDA/ANFs scaffold at 9:1 had low toxicity 62.81% which in the rage of

weak toxicity as referring to standard ISO 10993-5. This was shown that the PEGDA/ANFs novel scaffold is safe and non-toxic to be used as a function of tissue engineering scaffold

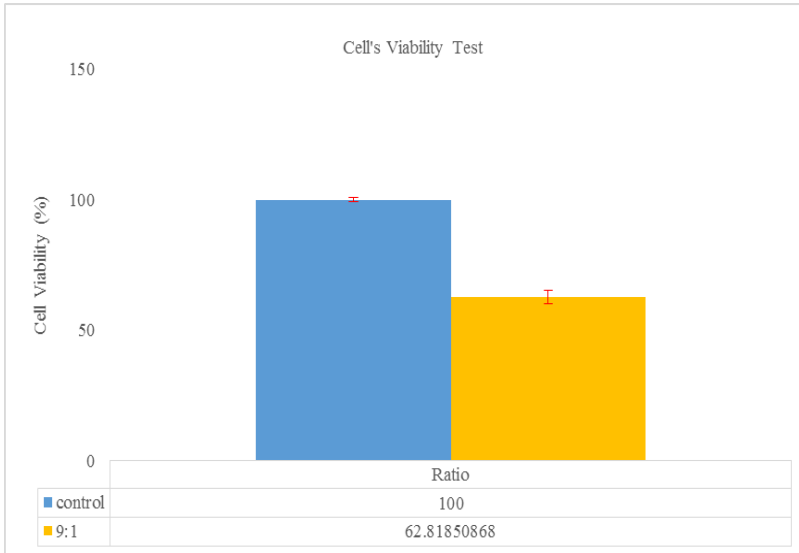

Figure 7: Cell viability of MTT assay for PEGDA/ANFs scaffold at ratio 9:1

PEGDA/ANFs Porous Structure Scaffold

In order to access the capability and potential of the novel biomaterials PEGDA/ANFs to print with porous structure under DLP 3D printing, the 3D scaffold with porous interior design were printed for composition bio-resin (1.0 %wt TPO-30% PEGDA) to ANFs at ratio 9:1, and 70s of curing time. Fig. 8 show the result of 3D printed scaffold with pores. The novel biomaterial resin of PEGDA filled with ANFs was successfully and able to print via DLP technique with precise pore size and better dimension structure. After post-curing, the sample of scaffold structure was observed become stiffer due to complete photopolymerization under post-curing process.

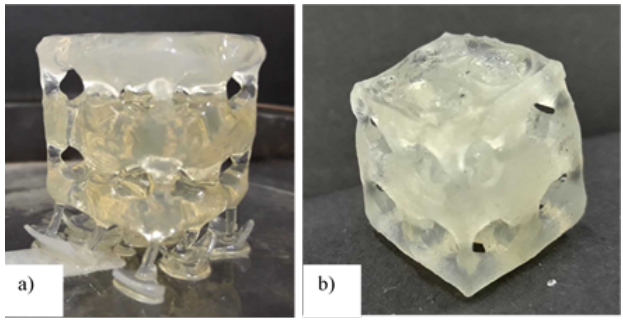

Figure 8: Cell 3D tissue engineering scaffold PEGDA/ANFs with porous structure; (a) before post curing (b) after post curing.

Conclusion

In the present work, it can be concluded that the fabrication of a novel 3D tissue engineering scaffold of PEGDA/ANFs with a perfect profile formation, dimension and pores was successfully printed. The use of photoinitiator TPO was identified can initiate the photopolymerization of PEGDA with ANFs under projector light condition ~405 nm. This study also proved the capability and has defined the feasible setting parameter of DLP printing machine to print a perfect 3D profile of the novel biomaterial PEGDA/ANFs as a function of tissue engineering scaffold which has not been reported up to date.

Acknowledgements

The authors wish to thank the Ministry of Higher Education (MOHE), Universiti Teknologi Malaysia (UTM) and Research Management Center, UTM for the financial support to this work through the Geran Universiti Penyelidikan (GUP) funding number Q.J130000.2524.20H47 and research grant under code R.J130000.7651.4C309. Many thanks to Universiti Kuala Lumpur for research funding under Short Term Research Grant (STRG 18038).

References

[1] W.-Y. Yeong, C.-K. Chua, K.-F. Leong, and M. Chandrasekaran, “Rapid prototyping in tissue engineering: challenges and potential,” Trends Biotechnol., vol. 22, no. 12, pp. 643–652, 2004.

[2] J. Henkel et al., "Bone Regeneration Based on Tissue Engineering Conceptions – A 21st Century Perspective," Nat. Publ. Gr., vol. 1, no. 3, pp. 216–248, 2013.
[3] D. Banoriya, R. Purohit, and R. K. Dwivedi, "Advanced Application of Polymer based Biomaterials," Mater. Today Proc., vol. 4, no. 2, pp. 3534–3541, 2017.
[4] Wang and K. W. K. Yeung, "Bone grafts and biomaterials substitutes for bone defect repair: A review," Bioact. Mater., 2017.
[5] J. R. Porter, T. T. Ruckh, and K. C. Popat, "Bone tissue engineering: A review in bone biomimetics and drug delivery strategies," Biotechnol. Prog., vol. 25, no. 6, pp. 1539–1560, 2009.
[6] K. F. Leong, C. K. Chua, N. Sudarmadji, and W. Y. Yeong, "Engineering functionally graded tissue engineering scaffolds," J. Mech. Behav. Biomed. Mater., vol. 1, no. 2, pp. 140–152, 2008.
[7] A. A. Osama and S. M. Darwish, "Fabrication of Tissue Engineering Scaffolds U sing Rapid Prototyping T echniques," Int. J. Ind. Manuf. Eng., vol. 5, no. 11, pp. 2317–2325, 2011.
[8] D. Liu, C. Yi, D. Zhang, J. Zhang, and M. Yang, "Inhibition of proliferation and differentiation of mesenchymal stem cells by carboxylated carbon nanotubes," ACS Nano, 2010.
[9] N. H. A. Ngadiman, A. Idris, M. Irfan, D. Kurniawan, N. M. Yusof, and R. Nasiri, "γ-Fe2O3 nanoparticles filled polyvinylalcohol as potentialbiomaterialfortissue engineering scaffold," J. Mech. Behav. Biomed. Mater., vol. 49, pp. 90–104, 2015.
[10] Z. Wei, X. Ma, M. Gou, D. Mei, K. Zhang, and S. Chen, "3D printing of functional biomaterials for tissue engineering," Curr. Opin. Biotechnol., vol. 40, pp. 103–112, 2016.
[11] K. Pluta, D. Malina, and A. Sobczak-kupiec, "Scaffolds for Tissue Engineering," Tech. Trans. Chem., vol. 1, no. 17, pp. 17–27, 2015.
[12] Q. Mu, G. Du, T. Chen, B. Zhang, and B. Yan, "Suppression of human bone morphogenetic protein signaling by carboxylated single-walled carbon nanotubes," ACS Nano, 2009.
[13] Y. Phanny and M. Todo, "Effect of Sintering Time on Microstructure and Mechanical Properties of Hydroxyapatite Porous Materials for Bone Tissue Engineering Application," Evergreen, vol. 1, no. 2, pp. 1–4, 2014.
[14] R. Gauvin et al., "Microfabrication of complex porous tissue engineering scaffolds using 3D projection stereolithography," Biomaterials, vol. 33, no. 15, pp. 3824–3834, 2012.
[15] R. Langer and J. P. Vacanti, "Tissue engineering," Science (80-.)., vol. 260, no. 5110, pp. 920–926, 1993.
[16] L. Moroni, J. Schrooten, R. Truckenmüller, J. Rouwkema, J. Sohier, and C. A. Van Blitterswijk, "Tissue Engineering: An Introduction," in Tissue Engineering: Second Edition, 2nd ed., Academic Press, 2014, pp. 1–21.

[17] A. Kantaros, N. Chatzidai, and D. Karalekas, “3D printing-assisted design of scaffold structures,” Int. J. Adv. Manuf. Technol., vol. 82, no. 1–4, pp. 559–571, 2016.
[18] J. An, J. E. M. Teoh, R. Suntornnond, and C. K. Chua, “Design and 3D Printing of Scaffolds and Tissues,” Engineering, vol. 1, no. 2, pp. 261–268, 2015.
[19] R. J. Mondschein, A. Kanitkar, C. B. Williams, S. S. Verbridge, and T. E. Long, “Polymer structure-property requirements for stereolithographic 3D printing of soft tissue engineering scaffolds,” Biomaterials, vol. 140, pp. 170–188, 2017.
[20] Z. Ning and X. Che, “Biofabrication of Tissue Scaffolds,” in Advances in Biomaterials Science and Biomedical Applications, R. Pignatello, Ed. InTech, 2013, pp. 315–328.
[21] B. Subia, J. Kundu, and S. C., “Biomaterial Scaffold Fabrication Techniques for Potential Tissue Engineering Applications,” Tissue Eng., no. 3, pp. 141–159, 2010.
[22] S. P. Singh, T. Bhardwaj, and M. Shukla, “Lattice modeling and finite element simulation for additive manufacturing of porous scaffolds,” IEEE Int. Conf. Adv. Mech. Ind. Autom. Manag. Syst., pp. 333–336, 2017.
[23] C. Lorandi, “A Smart Solution for Tissue Engineering Applications,” University of Trento, 2012.
[24] N. Alkhouli et al., “The mechanical properties of human adipose tissues and their relationships to the structure and composition of the extracellular matrix,” Am. J. Physiol. Metab., vol. 305, no. 12, pp. E1427–E1435, 2013.
[25] D. Lee, H. Zhang, and S. Ryu, “Elastic Modulus Measurement of Hydrogels,” in Cellulose-Based Superabsorbent Hydrogels, Springer International Publishing, 2018, pp. 1–21.
[26] ISO 10993-5, “A practical guide to ISO 10993-5: Cytotoxicity,” Med. Device Diagnostic Ind. Mag., pp. 2–4, 1998.
[27] G. J. López, M. Lehocký, P. Humpolíček, and P. Sáha, “HaCaT Keratinocytes Response on Antimicrobial Atelocollagen Substrates: Extent of Cytotoxicity, Cell Viability and Proliferation,” J. Funct. Biomater., vol. 5, no. 2, pp. 43–57, 2014.